

## Magnetic Circular Dichroism Studies of Carrier-Induced Ferromagnetism in $(\text{Ga}_{1-x}\text{Mn}_x)\text{As}$

B. Beschoten,<sup>1</sup> P. A. Crowell,<sup>1,2</sup> I. Malajovich,<sup>1</sup> and D. D. Awschalom<sup>1</sup>

<sup>1</sup>*Department of Physics, University of California, Santa Barbara, California 93106*

<sup>2</sup>*School of Physics and Astronomy, University of Minnesota, Minneapolis, Minnesota 55455*

F. Matsukura, A. Shen, and H. Ohno

*Laboratory for Electronic Intelligent Systems, Research Institute of Electronic Communication, Tohoku University, Sendai 980-77, Japan*

(Received 19 March 1999)

Magnetic circular dichroism is used to investigate the evolution of ferromagnetism in the  $p$ -type magnetic semiconductor  $(\text{Ga}_{1-x}\text{Mn}_x)\text{As}$ . Local Mn moments and holes produce two spectroscopically distinct contributions, whose properties reveal an antiferromagnetic Mn-hole alignment in the ferromagnetic state. These components are present in both metallic and insulating samples with different temperature and field dependences, suggesting that the holes play a more active role in mediating the ferromagnetic exchange than in traditional RKKY systems.

PACS numbers: 75.50.Pp, 75.50.Dd, 78.20.Ls

A distinguishing feature of diluted magnetic semiconductors (DMS's) is the coupling of electrons and holes to a population of local magnetic moments. This leads to a number of interesting properties, including an enhanced  $g$  factor for carriers [1] as well as novel excitations such as magnetic polarons [2]. Ferromagnetism, however, is rarely observed in semiconductors, which is a consequence of both the low density of carriers and the prevalence of antiferromagnetic superexchange among local moments. As a result, most ferromagnetic semiconductors are relatively exotic systems with low Curie temperatures [3–5]. The recent achievement of Curie temperatures over 100 K in the III-V DMS  $(\text{Ga}_{1-x}\text{Mn}_x)\text{As}$  at moderate Mn concentrations ( $x \sim 0.05$ ) is therefore particularly significant [6–8]. This material offers the possibility of exploiting traditional techniques for controlling the carrier population in a semiconductor in order to realize a new class of tunable ferromagnetic devices [9,10]. Identifying the role of charge carriers in the ferromagnetic exchange mechanism in  $(\text{Ga}_{1-x}\text{Mn}_x)\text{As}$  is therefore a high priority.

Here we present a systematic study of the magnetic circular dichroism (MCD) in  $(\text{Ga}_{1-x}\text{Mn}_x)\text{As}$  which identifies the critical role played by holes in the ferromagnetic exchange mechanism. We observe an unusual MCD signal comprising two contributions: a broad spectrum that scales with the thermodynamic magnetization of the sample and a narrower peak ( $\sim 150$  meV FWHM) which appears only in the ferromagnetic phase. We attribute this peak to the spontaneous spin splitting of the hole density of states. The sign of the peak indicates that the exchange between the holes and the local Mn moments is antiferromagnetic. We find ferromagnetism and the unusual MCD behavior in both metallic and insulating samples. This observation, along with the large spin polarization that can be inferred from transport measurements [11], suggests that the holes in  $(\text{Ga}_{1-x}\text{Mn}_x)\text{As}$  do not simply play the

role of a Fermi sea mediating a Ruderman-Kittel-Kasuya-Yosida (RKKY)-like exchange interaction.

The Mn in  $(\text{Ga}^{3+}_{1-x}\text{Mn}^{2+}_x)\text{As}$  functions as both a local moment and a  $p$ -type dopant, substituting for Ga at low concentrations  $x$ . Single phase  $(\text{Ga}_{1-x}\text{Mn}_x)\text{As}$  can be grown for  $x < 0.08$  using low-temperature molecular-beam epitaxy [6]. The structures for these experiments consist of 200 nm epilayers of  $(\text{Ga}_{1-x}\text{Mn}_x)\text{As}$ , each grown on a buffer layer of  $\text{Al}_{0.9}\text{Ga}_{0.1}\text{As}$  on semi-insulating GaAs (001). All of the samples are characterized by transport and SQUID magnetization measurements. Three of them have Mn concentrations  $x = 0.01$ , 0.035, and 0.053 with Curie temperatures  $T_c = 28$ , 62, and 101 K, respectively. The hole densities in all of these samples increase with Mn doping, but are  $\sim 10\%$  or less of the nominal Mn concentration in all cases. For the highest concentration sample,  $x = 0.053$ , the hole density is  $\sim 1.5 \times 10^{20} \text{ cm}^{-3}$  [11]. In the fourth sample ( $T_c = 20$  K), Si is codeposited at a Mn concentration of  $x = 0.01$ , partially compensating the holes with electrons.

The MCD measures the magnetic field-induced differential absorption  $\Delta = (\alpha^- - \alpha^+)/(\alpha^- + \alpha^+)$ , where  $\alpha^+$  and  $\alpha^-$  are the absorption coefficients for right and left circularly polarized light. The MCD and absorption are measured from 1.4 to 2.4 eV using a white light source and a monochromator. In order to perform all of these measurements in transmission, the GaAs substrate is removed from each sample by chemical etching. A magnetic field is applied parallel to the direction of light propagation and perpendicular to the plane of the sample.

Figure 1(a) shows the MCD spectra for the  $x = 0.053$  sample ( $T_c = 101$  K) at a field of  $B = 1$  T for temperatures from 5 to 130 K. A field sweep at  $E = 1.91$  eV and  $T = 5$  K is shown in the inset. The salient feature of these data is the broad peak structure centered at approximately 1.9 eV which occurs in both the ferromagnetic and

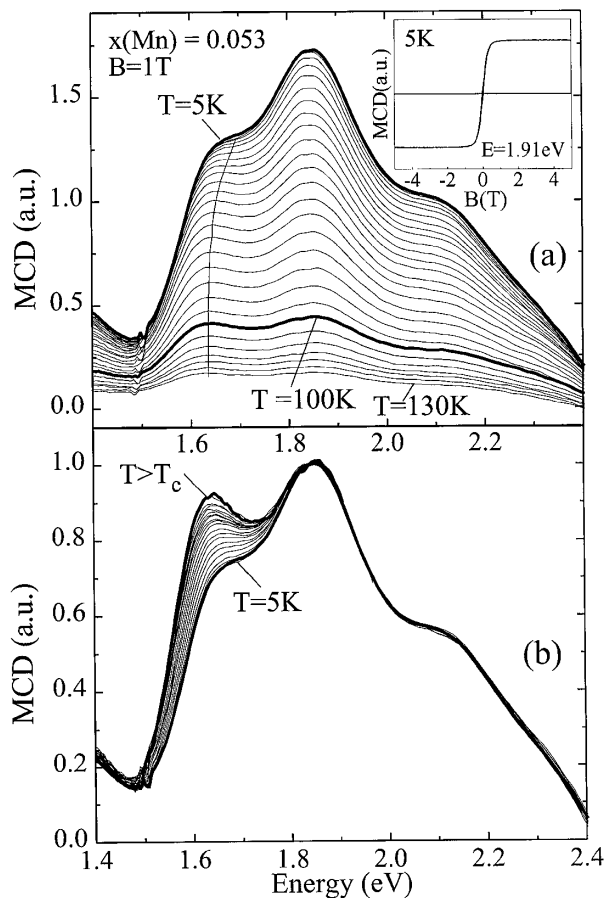


FIG. 1. Energy-dependent MCD of  $(\text{Ga}_{1-x}\text{Mn}_x)\text{As}$  as  $x = 0.053$ . (a) The MCD signal at  $B = 1$  T at different temperatures ranging from 5 K (top curve) to 130 K (bottom curve) in steps of 5 K. A field sweep at  $T = 5$  K and  $E = 1.91$  eV is shown in the inset. (b) MCD spectra taken from (a) normalized at 1.85 eV.

paramagnetic phases. Similar spectra are observed for all of the samples, and the MCD signal is positive over most of the energy range [12].

If the MCD signal is due entirely to an effective field proportional to the magnetization of the population of Mn moments, as is the case in traditional II-VI DMS [1], we expect the MCD data at a given energy to be proportional to the thermodynamic magnetization multiplied by a temperature-independent matrix element. This implies that the data at different temperatures should collapse onto a single curve when normalized by the thermodynamic magnetization or, equivalently, by the value of the MCD at a fixed energy. To test whether this is the case, we have scaled the MCD by dividing the data at each temperature by the value of the signal at 1.85 eV. The results of this normalization procedure are shown in Fig. 1(b). As expected, all data collapse to a single curve at all energies above  $T_c$ . For  $T < T_c$ , the data at high energies still fall on the same curve, while significant deviations are observed below 1.8 eV, where the magnitude of the relative MCD decreases. A clearer picture of this effect

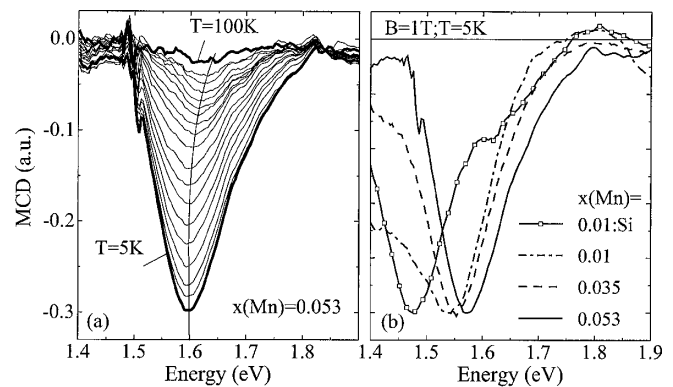


FIG. 2. Negative MCD signal for  $(\text{Ga}_{1-x}\text{Mn}_x)\text{As}$ . Panel (a) shows the temperature evolution for  $x = 0.053$ . The spectra are obtained from the normalized spectra shown in Fig. 1(b) as described in the text. (b) Doping dependence of the negative MCD peak at  $T = 5$  K and  $B = 1$  T for four different samples:  $x = 0.01 + \text{Si}$ ,  $x = 0.01$ ,  $x = 0.035$ , and  $x = 0.053$ . Each spectrum is normalized by its maximum value.

emerges if the high-temperature ( $T > T_c$ ) normalized data are subtracted from each of the curves in Fig. 1(b). The results of this subtraction procedure are shown in Fig. 2(a), which shows a negative peak that grows with decreasing temperature below  $T_c$ . The peak is limited to a small energy regime about 150 meV wide near the band edge energy of undoped GaAs. Like the positive MCD signal [Fig. 1(a)], the negative peak does not saturate at low temperatures.

The doping dependence of the negative peak is illustrated in Fig. 2(b), which shows a shift of the peak to higher energies with increasing carrier concentration. The spectra for each sample were obtained at  $T = 5$  K and  $B = 1$  T using the procedure outlined above. Each spectrum is normalized by its peak magnitude. In the  $x = 0.01$ , 0.035, and 0.053 samples, the hole concentration was increased by Mn doping alone. The Si-compensated sample has the smallest carrier concentration, and the energy of the MCD peak is the lowest of the group.

Figure 3 shows the temperature and magnetic field dependence of both the positive and negative contributions to the MCD at two different energies for all of the samples. The four upper panels show the MCD at 1.9 eV. These data represent the dominant background in each sample. The energies chosen for each of the lower panels correspond to the peak of the negative signal. In each case, the temperature dependence of the negative signal is distinct from that shown by the background. The difference is most dramatic in the Si-compensated sample, for which no negative signal (lower panels) is seen at high temperatures, even in high magnetic fields. In contrast, the background positive signal (upper panels) shows a prominent Curie-like tail as the magnetic field is increased. As the Mn doping is increased, the Curie tail in the positive signal decreases, and the difference in the temperature dependences of the two contributions to the MCD becomes less pronounced.

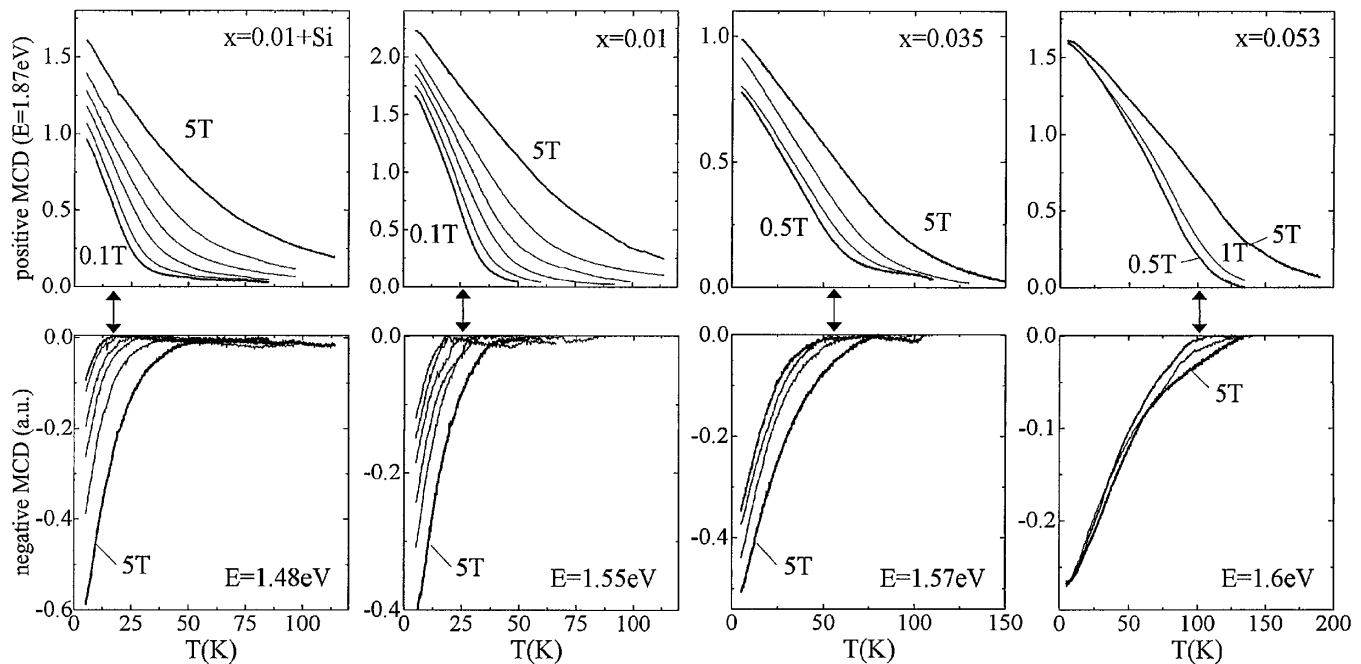


FIG. 3. Temperature dependence of the positive (Mn moment) (upper panels) and negative (hole) MCD signal (lower panels) at various magnetic fields:  $B = 0.1, 0.2, 0.5, 1.0, 2.0,$  and  $5.0$  T ( $x = 0.01 + \text{Si}$  and  $x = 0.01$ );  $B = 0.5, 1.0, 2.0,$  and  $5.0$  T ( $x = 0.035$ );  $B = 0.5, 1.0,$  and  $5.0$  T ( $x = 0.053$ ). The arrows indicate the Curie temperature  $T_c$  for each sample.

The data shown in Figs. 2 and 3 demonstrate that there are two distinct contributions to the MCD in  $(\text{Ga}_{1-x}\text{Mn}_x)\text{As}$ . The first is the spectrally broad positive background, and the second is the negative peak,  $\sim 150$  meV FWHM, which shifts to higher energies with increasing hole concentration. The temperature dependence of the positive background corresponds closely to that found in SQUID magnetization measurements, and so it is reasonable to assume that the positive MCD is proportional to the thermodynamic magnetization. We now focus on the negative peak: the proximity of this feature to the band gap (1.52 eV) of undoped GaAs as well as the evolution with hole concentration shown in Fig. 2(b) suggest that it is due to the spin splitting of the hole density of states. The origin of the spin splitting is the  $p$ - $d$  exchange between holes and localized Mn ions. This is similar to the  $p$ - $d$  exchange in II-VI semiconductors, except for the fact that the Mn, for which the electronic configuration is predominantly  $\text{Mn}^{2+}$  ( $3d^5$ ) at these concentrations [13], acts as both a  $p$ -type dopant and a local moment. The hole Fermi level increases with Mn concentration, leading to the shift in the negative MCD peak from 1.45 eV in the Si-compensated sample to 1.57 eV in the  $x = 0.053$  sample.

The sign of the negative peak indicates that the  $p$ - $d$  exchange is antiferromagnetic, assuming that the electron spin splitting is small compared to the heavy-hole spin splitting. This is similar to the case of II-VI DMS and is also consistent with the antiferromagnetic exchange observed for holes bound to  $\text{Mn}^{2+}$  in extremely dilute GaAs:Mn [14]. In contrast, the broad positive MCD

at higher energies has no clear analog in the II-VI DMS's.  $\text{Mn}^{2+}$  in zinc-blende II-VI DMS's generally has a band of intraion  $d$ - $d$  transitions in the range 2–3 eV [15], but these do not show strong magneto-optical activity. The MCD in  $(\text{Ga}_{1-x}\text{Mn}_x)\text{As}$ , for which we expect similar crystal-field splittings, is likely to be much larger since the ground state is spin polarized. We cannot, however, make any assignment of intraion transitions in this system without a greater knowledge of its electronic structure.

Another possible origin of the overall positive MCD has been noted recently by Szczytko *et al.* [16]. If the valence band structure of pure GaAs is preserved in  $(\text{Ga}_{1-x}\text{Mn}_x)\text{As}$ , then the absorption edge will shift from the center of the Brillouin zone to the Fermi wave vector, which will be different for the spin-down and spin-up heavy-hole bands. Assuming that the  $p$ - $d$  exchange is antiferromagnetic, a positive MCD signal can occur in this case if the combined dispersion of the conduction and valence bands at  $k_F$  exceeds their spin splitting. The presence of a negative MCD signal at lower energies could also be accommodated in this model by accounting for the depopulation of the light-hole band with increasing magnetic field. It is not clear, however, why the light-hole contribution should produce a spectrally narrow peak while the heavy-hole contribution is so broad. This could reflect the likelihood that the dispersion of the hole bands at these doping levels is no longer parabolic. Furthermore, in this model we would expect the heavy-hole contribution to the MCD to change sign from positive to negative as the doping is increased, but we find instead

that the overall signal remains positive down to the lowest Mn concentrations ( $x = 3 \times 10^{-4}$ ) that we have studied.

We therefore consider the most likely origin of the positive signal to be the Zeeman splitting of intraion transitions as discussed above. The negative peak is due to the antiferromagnetic  $p$ - $d$  exchange between hole spins and the  $\text{Mn}^{2+}$  ions. However, this assignment alone does not provide an explanation for the unusual temperature dependence shown in Fig. 3. In a typical II-VI DMS, for example, we expect the strength of the  $p$ - $d$  exchange interaction to be proportional to the total  $\text{Mn}^{2+}$  moment [1]. If that were the case here, the temperature dependence in the upper and lower panels of Fig. 3 would be the same. Although we expect the proportionality to break down in the limit of large hole spin polarizations, the data of Fig. 3 are most anomalous at high temperatures and lower carrier densities, for which the induced hole polarization is small. In all cases, the onset of the negative signal is correlated more closely with the Curie temperature (shown with arrows) than with the paramagnetic behavior observed for the positive MCD.

This anomalous temperature dependence indicates that the spin polarization of holes in  $(\text{Ga}_{1-x}\text{Mn}_x)\text{As}$  is not simply proportional to the number of  $\text{Mn}^{2+}$  moments. This is distinct from the behavior expected in traditional RKKY systems [17], in which local magnetic moments induce a spin polarization in a sea of free carriers by short-range exchange interactions. This discrepancy could be due in part to the large value of the spin splitting [9,11], which is comparable to the Fermi energy, and so the perturbative picture usually applied to RKKY systems is not appropriate in  $(\text{Ga}_{1-x}\text{Mn}_x)\text{As}$ . Although an extension of the RKKY approach to the case of large spin polarizations is possible [18], the difference in the temperature dependence of the two components of the MCD is largest when the hole spin polarization is smallest. The fact that the temperature dependence of the negative peak does not follow the positive MCD may indicate a separate hole-hole exchange mechanism in addition to the Mn-hole exchange [8]. Furthermore, we observe ferromagnetism in insulating samples, indicating that a population of free carriers is not necessary for ferromagnetism to occur in  $(\text{Ga}_{1-x}\text{Mn}_x)\text{As}$ .

Another possible origin for the different temperature dependence of the hole and Mn polarizations, particularly at low carrier concentration, is a feedback mechanism in which spatially localized hole states lower their energy by inducing a polarization cloud in a group of  $\text{Mn}^{2+}$  ions, forming a bound magnetic polaron. In this case, the alignment of Mn moments by an external field reduces the hole binding energy, thus increasing the size of the polaron [2]. The resulting increase in the  $\text{Mn}^{2+}$

polarization leads to the strong magnetic field dependence observed in the MCD of the insulating samples. A large negative magnetoresistance at low temperatures observed in these samples is consistent with this picture [19]. This polaronic model might also explain the enhanced paramagnetism in the insulating samples above  $T_c$ , since the effective moment of the polaronic complex is larger than that of an isolated spin. The model, however, cannot provide a description of the ferromagnetic state. As seen by the strong field dependence at low temperature, the relative number of ferromagnetically coupled  $\text{Mn}^{2+}$  moments is reduced with decreasing Mn content. This persistence of ferromagnetism in the insulating regime is one of the most intriguing characteristics of  $(\text{Ga}_{1-x}\text{Mn}_x)\text{As}$ .

We would like to thank S.J. Allen, D. Hone, and W. Kohn for helpful discussions. This work was supported by the AFOSR F46920-99-1-0033, the ONR N00014-99-1-0077, the NSF DMR-9701072, the JSPS Research for the Future program, and the Spin-Controlled Semiconductor Nanostructure program from the Ministry of Education, Japan. B.B. acknowledges the support of the Alexander von Humboldt Foundation V-3-FLF-1052866.

- 
- [1] J.A. Gaj, in *Diluted Magnetic Semiconductors*, edited by J.K. Furdyna and J. Kossut (Academic Press, Boston, 1988).
  - [2] S. von Molnár and T. Penney, in *Localization and Metal-Insulator Transitions*, edited by H. Fritzsche and D. Adler (Plenum Press, New York, 1985).
  - [3] T. Story *et al.*, Phys. Rev. B **42**, 10477 (1990).
  - [4] H. Munekata *et al.*, Phys. Rev. Lett. **63**, 1849 (1989).
  - [5] A. Haury *et al.*, Phys. Rev. Lett. **79**, 511 (1997).
  - [6] H. Ohno *et al.*, Appl. Phys. Lett. **69**, 363 (1996).
  - [7] T. Hayashi *et al.*, J. Cryst. Growth **175–176**, 1063 (1997).
  - [8] A. Van Esch *et al.*, Phys. Rev. B **56**, 13 103 (1997).
  - [9] H. Ohno *et al.*, Appl. Phys. Lett. **73**, 363 (1998).
  - [10] H. Ohno, Science **281**, 951 (1998).
  - [11] F. Matsukura *et al.*, Phys. Rev. B **57**, R2037 (1998).
  - [12] The detailed spectral structure of the MCD signal is affected by interference fringes due to etaloning in the sample. These do not influence the field and temperature dependences.
  - [13] J. Okabayashi *et al.*, Phys. Rev. B **58**, R4211 (1998).
  - [14] J. Schneider *et al.*, Phys. Rev. Lett. **59**, 240 (1987); M. Baeumler *et al.*, Mater. Sci. Forum **38–41**, 797 (1989).
  - [15] J.F. MacKay *et al.*, Phys. Rev. B **42**, 1743 (1990).
  - [16] J. Szczytko *et al.*, Phys. Rev. B **59**, 12 935 (1999).
  - [17] M.A. Ruderman and C. Kittel, Phys. Rev. **96**, 99 (1954).
  - [18] T. Dietl, A. Haury, and Y. Merle d'Aubigné, Phys. Rev. B **55**, R3347 (1997).
  - [19] F. Matsukura *et al.* (unpublished).